

RINOPOLYCRETE - TOWARDS A CEMENT-FREE AND FULLY RECYCLED CONCRETE



PROJECTO FCT

PTDC/ECI-COM/29196/2017

## **Recycled inorganic polymer concrete - Towards a cement-free and fully recycled concrete**

### **(RInoPolyCrete)**

#### **Task 1**

**Literature review on the influence of municipal solid waste incinerator bottom ash  
on the performance of alkali-activated materials**

May, 2019

Financiamento FCT/POCI



Governo da República Portuguesa



União Europeia FEDER

**FCT** Fundação para a Ciência e a Tecnologia

MINISTÉRIO DA CIÊNCIA E DO ENSINO SUPERIOR

Portugal



**CERIS** : Civil Engineering Research  
and Innovation for  
Sustainability

## Table of contents

1. Introduction	1
2. Chemical and physical characteristics of MIBA	1
3. Performance of MIBA-based alkali-activated materials	4
3.1. Fresh state performance	4
3.2. Mechanical performance	5
3.3. Durability performance	8
3.4. Microstructure	11
3.5. Toxicity	13
4. Final remarks	14
References	14

## List of Figures

Figure 1 - Ternary diagram ( $\text{SiO}_2$ - $\text{CaO}$ - $\text{Al}_2\text{O}_3$ ) of MIBA [2] .....	3
Figure 2 - SEM images of MIBA particle (a) 2000 and (b) 5000 x (Chen et al., 2016) ..	3
Figure 3 - Effect of thermally treated and untreated MIBA on the setting time of pastes [10] .....	4
Figure 4 - Effect of liquid to solid ratio and mix duration of the strength of alkali-activated MIBA paste [13] .....	5
Figure 5 - Influence of liquid to solid ratio and mix duration on density of alkali-activated MIBA [13] .....	10
Figure 6 - Relationship between microstructure and strength of the alkali-activated MIBA [13] .....	10
Figure 7 - Effect of MIBA on the micro structure of cement and geopolymer mortar ..	11
Figure 8 - XRD diffractograms of MIBA and alkali-activated MIBA paste [17] .....	13

## List of Tables

Table 1 - Studies related to alkali-activated construction materials made with MIBA.... 9

### **Acronyms:**

AAM - alkali activated materials

FA - fly ash;

GGBS - ground granulated blast furnace slag;

MIBA - municipal solid waste incinerator bottom ash;

MIFA - municipal incinerated fly ash;

OPC - ordinary Portland cement;

SCM - supplementary cementitious materials.

## 1. Introduction

This report presents the findings of the literature review expected of Task 1 within the scope of the FCT Project ECI-COM/29196/2017- “Recycled inorganic polymer concrete - Towards a cement-free and fully recycled concrete (RIInoPolyCrete)”. The main aim of this literature review is to demonstrate the influence of using municipal solid waste incinerator bottom ash (MIBA) as solid precursor on the performance of alkali-activated materials (AAM).

The construction industry is one of the economic sectors with the highest environmental impacts, in terms of extracted natural resources, energy consumption and emissions released into the biosphere. The sector’s materials with the highest environmental impact is cement, since it is one of the most widely used construction materials in the World and releases a considerable amount of carbon dioxide during its production. To reduce the use of this material, it has been suggested that by-products, such as sewage sludge ash, biomass ash or MIBA should be used as partial cement replacement. Techniques such as alkali activation of waste aluminosilicate precursors have also been considered as a viable alternative for the complete substitution of cement in the production of mortars and concrete. One of such wastes is MIBA. In the case of Portugal, about five million tonnes of municipal solid waste (MSW) are produced every year, in which around one million metric tonnes are incinerated [1]. Valorsul’s MSW incineration unit produces around one hundred thousand metric tonnes of MIBA per year, treating most of Lisbon’s MSW. There is insufficient demand for this material and, as a result, most of it is deposited in huge heaps, reshaping significantly the landscape of Mato da Cruz landfill, in Lisbon’s outskirts. Additionally, given the scarcity of outlets for MSW ashes, there is significant scope for developing value-added applications for them. These issues can be overcome with their alkali-activation to produce new binding systems.

## 2. Chemical and physical characteristics of MIBA

Alkali activators, such as sodium hydroxide and sodium metasilicate, react with amorphous  $Al_2O_3$  and  $SiO_2$  present in the solid precursor, resulting in a solid inorganic polymer showing

properties comparable to those of hydrated cement. It is widely known that the chemical composition of the precursor has a considerable influence on the performance of its resulting AAM. Some of this report's authors have collected significant amount of data in a previous study [2]. The findings showed that  $\text{SiO}_2$  usually is the predominant component, followed by  $\text{CaO}$ ,  $\text{Al}_2\text{O}_3$  and  $\text{Fe}_2\text{O}_3$ ,  $\text{P}_2\text{O}_5$ ,  $\text{MgO}$ , and  $\text{K}_2\text{O}$  with average contents of 37%, 22%, 10%, 8%, 3%, 3%, 2%, 2% and 1%, respectively. However, there was a notable scatter, which can be explained by the considerable variability of MSW.

Figure 1 presents the ternary diagram  $\text{SiO}_2$  -  $\text{CaO}$  -  $\text{Al}_2\text{O}_3$  of MIBA of 187 samples. Most of the samples are divided between the “pozzolanic regions” and the “latent hydraulic”. Apart from limestone, cement and ground granulated blast furnace slag (GGBS), MIBA has higher  $\text{CaO}$  content than other SCM (e.g. coal fly ash, brick feedstock, silica fume and natural pozzolan). Nevertheless, the oxide composition is indicative of the materials' contents, but not of its pozzolanicity/reactivity, since many of its phases are crystalline. Furthermore, most of MIBA's aluminium-containing phases are likely to be in its purest metallic form, which is known to have corrosion reactions in alkali environments. It has been suggested that MIBA can be defined as a silica-based powder due to its high  $\text{SiO}_2$  content coming from discarded soda-lime-silicate glass [3]. Concerning the  $\text{Si}/\text{Al}$  and  $\text{Na}/\text{Al}$  ratios, it has been reported that these must be in range of 1.8-2.5 and 0.9-1.2, respectively, for optimum performance since the presence of Al is detrimental [4, 5].

According to the database made by Dhir *et al.* [2], ranges for the specific gravity and moisture content of MIBA were identified as 2.24-2.78% and 12-18%, respectively. MIBA particles have irregular and angular shape with a porous microstructure that forms during the incineration process due to the formation of gasses (Figure 2).

After incineration, MIBA present particle size distribution like that of “all-in” aggregates. However, previous studies have shown that, after being submitted to a milling process, MIBA can present a particle size distribution similar to that of Portland cement [6-9].



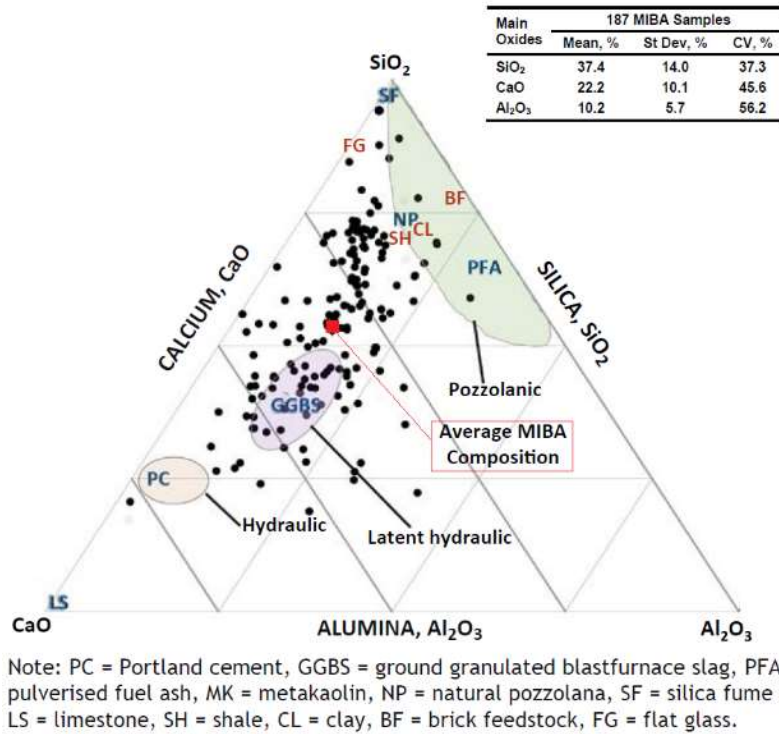


Figure 1 - Ternary diagram (SiO<sub>2</sub> - CaO - Al<sub>2</sub>O<sub>3</sub>) of MIBA [2]

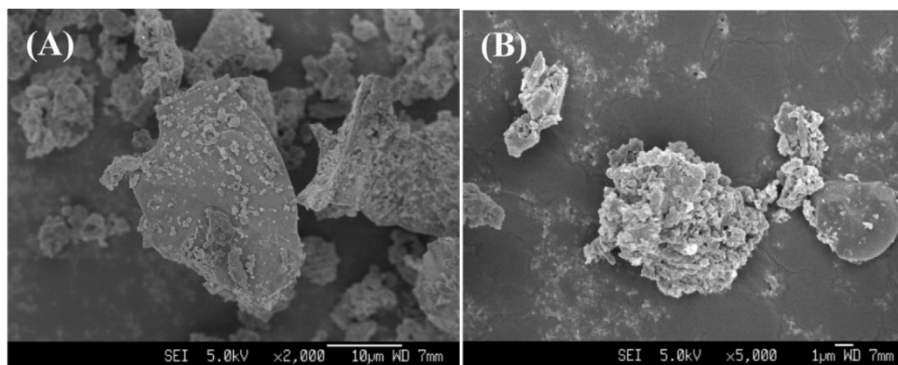


Figure 2 - SEM images of MIBA particle (a) 2000 and (b) 5000 x (Chen et al., 2016)

### 3. Performance of MIBA-based alkali-activated materials

#### 3.1. Fresh state performance

In comparison with OPC pastes, the setting times of alkali-activated pastes made with untreated MIBA are likely to be much higher [10, 11]. However, the setting time can be lowered by treating MIBA by exposure to high temperatures (Figure 3). In some cases, the setting time of the alkali-activated paste is very short. In the study of Garcia-Lodeiro *et al.* [12], a hybrid cement was manufactured by blending 40% of alkali activated MSW ashes and 60% of OPC. About 5% of sulphate-bearing compounds ( $\text{Na}_2\text{SO}_4$  and  $\text{CaSO}_4$ ) were added to the mix to control the system's setting.

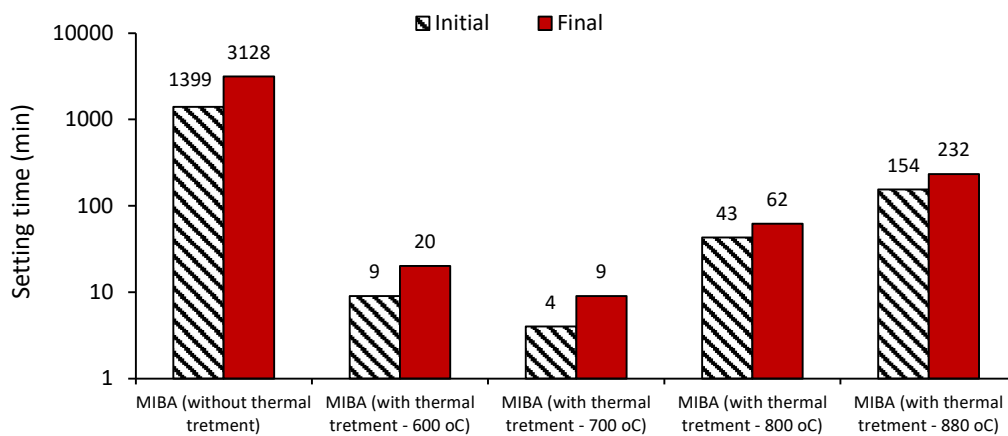


Figure 3 - Effect of thermally treated and untreated MIBA on the setting time of pastes [10]

Tang *et al.* [8] mixed treated MIBA with cement at a ratio of 3:7 to produce hybrid alkali-activated mortar. They concluded that, relatively to conventional mortar (170 mm), the use of MIBA led to a decrease of the mortar's flowability (160-169 mm). Regarding the heat of hydration, the same authors showed that the maximum heat release rate of MIBA pastes was 20% to 30% lower than that of the cement paste.

### 3.2. Mechanical performance

According to the results of previous studies [10, 11, 13, 14], the average strength of alkali-activated paste containing MIBA was 2.3 MPa. For this reason, several attempts have been made to overcome this issue. Chen et al. [13] showed that increasing the mixing time (15, 30, 60 and 120 minutes) generally resulted in higher compressive strength (Figure 4). Mixing the alkaline solution with the precursor for 60 minutes was found to be optimum in terms of compressive strength and porosity, as it would potentiate the metallic aluminium's reaction and reduce the existence of hydrogen-filled voids in the resulting mortars. Furthermore, the authors used sodium hydroxide solution as an activator with molar concentration varying from 2 M to 16 M and concluded that 8 M was the optimum concentration.

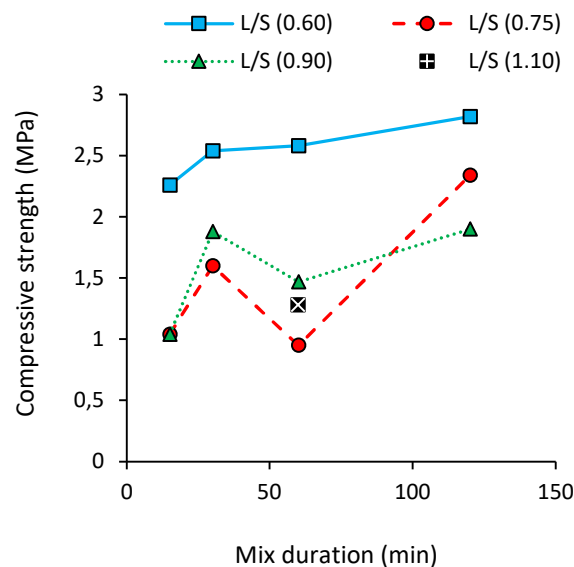


Figure 4 - Effect of liquid to solid ratio and mix duration of the strength of alkali-activated MIBA paste [13]

Galiano *et al.* [14] produced alkali-activated pastes with a constant composition of FA and MIBA, and various contents of OPC, lime, water, potassium hydroxide, sodium silicate, potassium silicate, kaolin, metakaolin and GGBS. The compressive strength of the samples varied

between 1 MPa and 9 MPa. The authors suggested that lime should be incorporated in such mixes due to the higher potential for strength development.

Qiao *et al.* [10, 11] produced alkali-activated pastes made with untreated and thermally treated MIBA (heated up to 880 °C). In both cases, the macro-porosity was considered one of the reasons for achieving low-strength samples (up to 2.8 MPa). This increase in porosity was due to the formation of hydrogen gas from the reaction of aluminium under high pH conditions ( $\text{Al} + 2\text{OH}^- + 2\text{H}_2\text{O} \rightarrow \text{H}_2 + \text{Al}(\text{OH})_4^-$ ). To overcome this issue, the authors proposed a new method to obtain higher strength (13-15 MPa) by pressing the samples. A similar technique (preparing alkali-activated MIBA samples with a load of 5 MPa) was used in the study of Rožek *et al.* [15], wherein higher strength was achieved. In their study, the CaO/SiO<sub>2</sub> molar ratio was modified to 0.83 by using silica (as grained quartz) or calcium oxide (pure) as partial replacement of precursor (untreated MIBA). The modification method increased the strength of alkali-activated MIBA sample from 24 MPa to 75 MPa. However, the samples were pressed at 5 MPa to eliminate the air bubbles and then subjected to hydrothermal treatment under saturated-steam pressure at 180 °C for 10 hours.

Zhu *et al.* [16, 17] studied the characteristics of pastes made with MIBA, water glass and sodium hydroxide. The average compressive strength of the samples was 3 MPa. The authors concluded that the samples comprised 30% of C-S-(A)-H and other polymer gels. The same authors in another study [18] demonstrated increased strength in alkali-activated pastes (~70 MPa), by increasing the SiO<sub>2</sub>/Na<sub>2</sub>O ratio of the activating solution from 0 to 1.2. The solution made with water glass (Merck; H<sub>2</sub>O 65%, SiO<sub>2</sub> 27% and Na<sub>2</sub>O 8%), sodium hydroxide (14 M), salicylic acid (Sigma-Aldrich; purity > 99%), hydrochloric acid (Sigma-Aldrich; concentration 37 wt.%) and methanol (Merck; purity > 99.9%) were used in the chemical extractions.

Kim and Kang [19] focused the effect of sodium hydroxide molarity, particle size of MIBA and liquid/solid ratio on the compressive strength of alkali-activated MIBA, which was previously vitrified. The strength increased with decreasing size of precursor and increasing molar concentration

(up to 20 M). The optimum liquid/solids ratio was 0.13. Similarly to the study of Rožek *et al.* [15], the samples were pressed ( $316 \text{ kg/cm}^2$ ) to obtain high strength.

Wongsa *et al.* [20] studied the possibility of incorporating MIBA as a replacement material for FA type C (high calcium) to produce alkali-activated mortar. According to the pore size distribution results, porosity, compressive strength and SEM, the incorporation at 20% of MIBA with FA is optimum to be used as a precursor for alkali-activated mortar. However, the strength of the mortar with 40% of MIBA was higher than that of the control mortar.

Huang *et al.* [21] produced alkali-activated mortar and focused on the active components of the precursor. The percentage of  $\text{SiO}_2$  (MIBA) and CaO (ground blast furnace slag) were high. The compressive strength of the samples was low due to the low active silica content, which affects the growth and formation of C-A-S-H and C-S-H. To overcome this issue, the authors incorporated a constant amount of sodium hydroxide and various amounts of liquid and solid sodium silicate. The compressive strength increased with increasing amount of solid sodium silicate up to 0.13 (sodium silicate/precursor mass ratio). Additionally, the strength of the mortars could further increase with the use of the liquid sodium silicate (up to 0.27). Higher percentages of sodium silicate may negatively affect the strength of alkali-activated mortars because they may provide activated sodium and silica in excess, which causes the precipitation of magadiite (with large quantities of active sodium, C-A-S-H decreases because the active sodium consumes large quantities of active aluminium and as a result form N-A-S-H gels).

Huang *et al.* [22] mixed both sodium hydroxide (4.8 M) and sodium silicate (2.6 M) as alkaline solution to produce standard mortar samples by using MIBA and GGBS. The strength of the samples was between 28 MPa and 53 MPa, depending on the curing method (natural, standard room, seal, steam and soaking curing). The authors showed that the standard and soaking curing methods were not suitable for strength development of the AAM because both curing methods leach out free alkali and  $\text{OH}^-$ , and other beneficial elements. Therefore, the authors concluded

that the best curing method for the AAM is seal curing because most of the beneficial substances of the samples remain.

Garcia-Lodeiro *et al.* [12] produced mortar by blending 40% MSW ashes and 60% OPC. The strength of the mortar was about 33 MPa.

Xuan *et al.* [23] studied the mechanical behaviour of concrete made with both alkali activated MIBA and glass. The strength of samples was between 1 MPa and 10 MPa. The incorporation of glass did not show a promising result. However, the concrete mix containing 20% of glass exhibited low thermal conductivity.

Similar to the compressive strength, the tensile strength of alkali-activated pastes (0.6-2.8 MPa) and mortar (0.2-0.65 MPa) containing MIBA is normally low [10, 24].

### 3.3. Durability performance

Most of the literature focused on the microstructure (e.g. density, porosity and air voids) of alkali-activated samples made with MIBA. Other essential durability properties have not been studied yet (Table 1).

Chen *et al.* [13] studied the dry density of alkali-activated paste made with MIBA. The authors reported that the lower density (600-1000 kg/m<sup>3</sup>) of the sample is related to the hydrogen gas from the reaction between the precursor's aluminium fraction and the alkaline solution. In addition, the authors studied the effect of liquid to solid ratio and mix duration on the dry density and porosity of the samples. The results show that the density increases with increasing the mixing time (Figure 5). Further details regarding the issue of Al can be seen in the study of Song *et al.* [7]. Figure 5 also shows that the dry density of the samples increases with decreasing liquid to solid ratio. The authors reported that higher liquid to solid ratio not only increases porosity but also accelerates the rate of hydrogen gas.

Table 1 - Studies related to alkali-activated construction materials made with MIBA

NO.	Study	Sample	Tests										Others			
			Compressive strength	Toxicity	XRD <sup>a</sup>	SEM <sup>b</sup>	FT-IR <sup>c</sup>	XRF <sup>d</sup>	Density-Porosity	Conductivity - Heat	Setting time - Hydration	PH		Tensile strength		
1	Zhu <i>et al.</i> [18]	Paste	X	-	X	-	X	-	-	-	-	-	-	-	-	NMR <sup>e</sup>
2	Rožek <i>et al.</i> [15]	Paste	X	X	X	X	X	X	X	-	-	-	-	-	-	Raman spectra
3	Zhu <i>et al.</i> [17]	Paste	X	-	X	-	X	X	X	-	-	-	-	-	-	-
4	Giro-Paloma <i>et al.</i> [3]	Paste	-	X	X	X	X	X	-	-	-	X	-	-	-	TGA <sup>f</sup>
5	Chen <i>et al.</i> [13]	Paste	X	X	X	X	X	-	X	-	-	-	-	-	-	-
6	Zhu <i>et al.</i> [16]	Paste	X	-	-	-	X	X	X	-	-	-	-	-	-	NMR <sup>e</sup>
7	Song <i>et al.</i> [7]	Paste	X	-	X	X	-	-	X	-	-	-	-	-	-	Hydrogen generation; Shrinkage
8	Kim and Kang [19]	Paste	X	-	X	X	-	-	-	-	-	-	-	-	-	-
9	Lancellotti <i>et al.</i> [25]	Paste	-	X	X	X	X	-	-	X	-	-	-	-	-	EDS <sup>g</sup>
10	Krausova <i>et al.</i> [26]	Paste	-	X	X	X	-	-	X	-	-	X	-	-	-	-
11	Galiano <i>et al.</i> [14]	Paste	X	X	-	-	-	-	-	-	-	X	-	-	-	-
12	Onori <i>et al.</i> [27]	Paste	X	X	X	X	X	X	X	-	-	X	-	-	-	TAG <sup>f</sup>
13	Qiao <i>et al.</i> [10]	Paste	X	-	X	X	-	X	-	-	X	-	-	-	-	Release of gas
14	Qiao <i>et al.</i> [11]	Paste	X	X	X	X	-	-	X	-	X	-	-	-	-	-
15	Huang <i>et al.</i> [21]	Mortar	X	-	X	X	X	-	-	-	-	-	-	-	-	Active silica content; EDS <sup>g</sup>
16	Huang <i>et al.</i> [22]	Mortar	X	X	X	X	X	-	-	-	-	X	-	-	-	-
17	Liu <i>et al.</i> [28]	Mortar	X	-	X	-	-	-	X	-	-	-	-	-	-	Release of gas
18	Wongsa <i>et al.</i> [20]	Mortar	X	-	X	X	X	-	X	-	-	-	-	-	-	-
19	Tang <i>et al.</i> [8]	Mortar	X	X	X	X	-	X	-	X	-	-	X	-	-	MALCBA <sup>h</sup> ; Flow of mortar mix
20	Garcia-Lodeiro <i>et al.</i> [12]	Mortar	X	X	X	X	-	-	-	-	-	-	X	-	-	-
21	Jing <i>et al.</i> [24]	Mortar	-	X	X	X	-	-	X	-	-	-	-	X	-	-
22	Penilla <i>et al.</i> [29]	Mortar	-	-	X	X	X	-	-	-	-	-	-	-	-	-
23	Xuan <i>et al.</i> [23]	Concrete	X	-	X	X	X	X	X	X	-	-	-	-	-	EDS <sup>g</sup>

<sup>a</sup> XRD - X-rays Diffraction; <sup>b</sup> SEM - Scanning Electron Microscope; <sup>c</sup> Ft-IR - Fourier transform infrared spectroscopy; <sup>d</sup> XRF - X-rays Fluorescence; <sup>e</sup> NMR is a powerful characterization technique to identify chemical structure of amorphous gel and has been used to analyse cement and geopolymer nano-structures; <sup>f</sup> TGA - Thermogravimetric analysis; <sup>g</sup> EDS - Energy Dispersive X-Ray Spectroscopy <sup>h</sup> MALCBA - Metallic aluminium content of bottom ash samples (Metallic Aluminium (Al<sup>0</sup>) Quantification).

Figure 6 shows the relationship between the dry density, porosity, and compressive strength of the pastes. The results show that there is a strong relation between strength and both porosity and density of the samples. Therefore, it is important to solve the issue of hydrogen formation in order to obtain high strength sample.

Qiao *et al.* [11] obtained alkali-activated MIBA with a bulk density of 2000 kg/m<sup>3</sup> by pressing the sample. Rožek *et al.* [15] also showed the advantage of pressing technique in terms of a denser microstructure (2350 kg/m<sup>3</sup>). Jing *et al.* [24] showed a relationship between bulk density,

tensile strength with the compaction pressure on the alkali-activated mortars with MIBA and confirmed the necessity for a pressing technique.

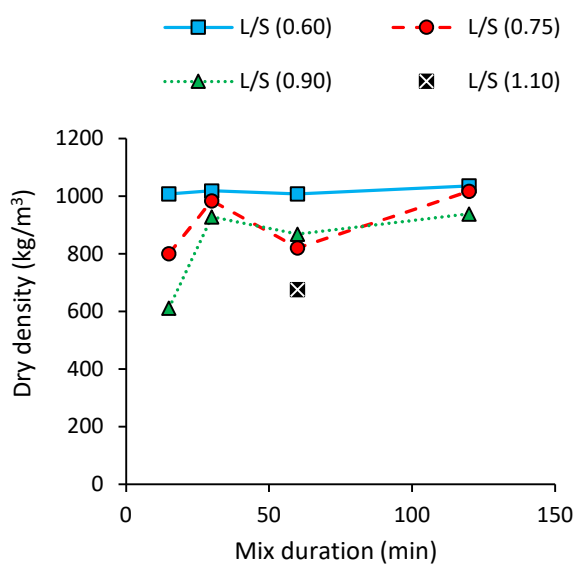


Figure 5 - Influence of liquid to solid ratio and mix duration on density of alkali-activated MIBA [13]

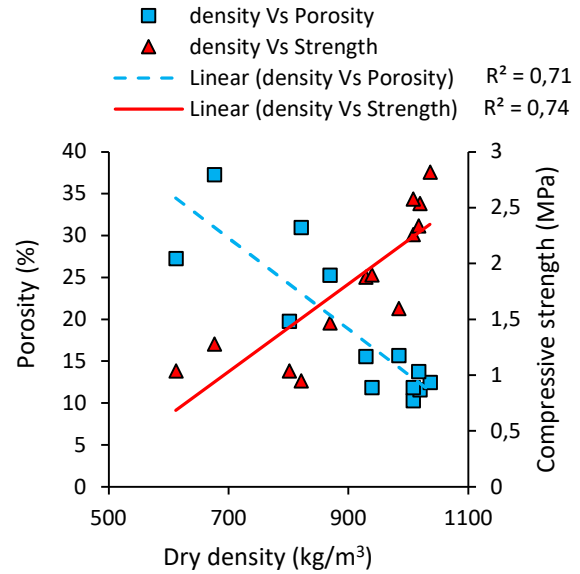


Figure 6 - Relationship between microstructure and strength of the alkali-activated MIBA [13]

Zhe *et al.* [16, 18] showed that the dry density of alkali-activated paste containing MIBA was low (900-1100 kg/m<sup>3</sup>) due to hydrogen formation.

Krausova *et al.* [26] mixed various ratio of glass powder (10-30%) with MIBA and then thermally treated with different temperatures. The results showed that the incorporation of 10% glass powder with and without thermal treatment (700 °C/1h) was optimum for higher dry densities. The authors also showed that the water absorption increased as the temperature increased. However, the effect of temperature on specific gravity depended on the incorporation ratio of MIBA. The SEM images showed that the samples' porosity without heat treatment was lower than that of those with the treatment. This means that the thermal treatment is not a proper approach to



eliminate the gas generated due to the oxidation of Al. In addition, the water absorption rate sharply decreased with increasing waste glass powder and heat treatment.

Wongsa *et al.* [20] compared the porosity, air voids, capillary pores and gel pores of cement and alkali-activated mortar (Figure 7). According to the mentioned characteristics and SEM, the incorporation at 20% of MIBA with FA is optimum to be used as a precursor for alkali-activated mortar because it increases the homogeneity and density.

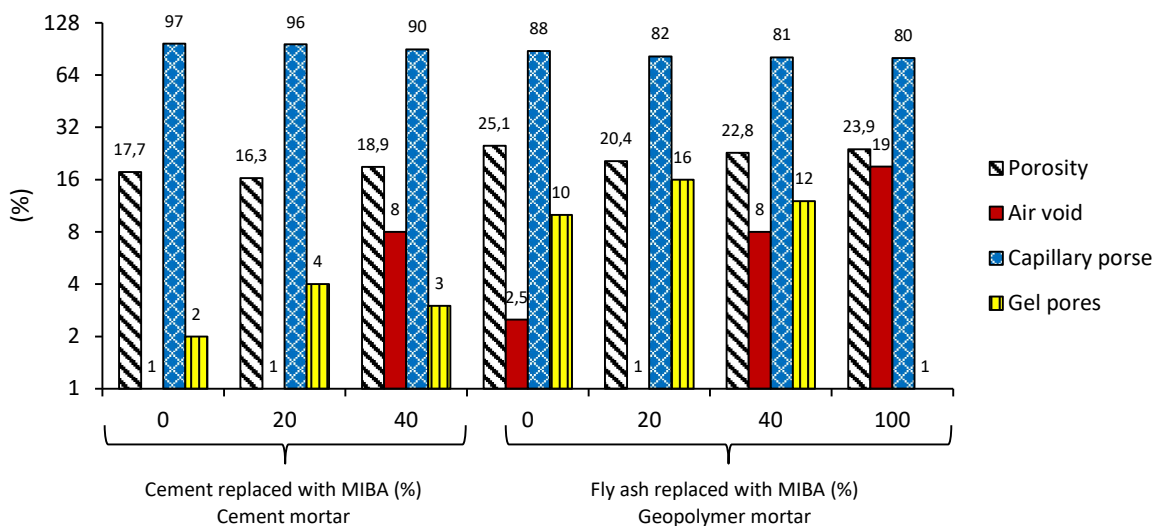


Figure 7 - Effect of MIBA on the micro structure of cement and geopolymer mortar [20]

### 3.4. Microstructure

Apart from the toxicity and compressive strength of AAM containing MIBA, their microstructure (e.g. XRD, SEM, FT-IR and XRF) is also one of the properties that researchers focused on (Table 1). Giro-Paloma *et al.* [3] performed SEM analysis on alkali activated MIBA paste and reported a low-density microstructure in spite of the presence of inorganic polymers. Additionally, there were unreacted MIBA particles even though the samples were cured for 15 days.

Qiao *et al.* [10] also confirmed that alkali-activated MIBA pastes usually are a low compacted

granular material with diminutive evidence of hydration. Additionally, the authors showed an extensive evidence of hydration-products particularly C-S-H gel and denser microstructure for the samples made with thermally treated MIBA. The same authors [11] showed that the air bubbles caused by hydrogen gas can be eliminated by mixing thermally treated MIBA with 10% of hydroxide calcium. SEM showed that, unlike coal FA particles (smooth glassy spherical surface), MIBA particles are irregular and rough because of low incineration temperatures ( $\sim 800$  °C) that are under the melting temperature of the majority of the minerals [13].

Giro-Paloma *et al.* [3] studied alkali-activated MIBA paste by FT-IR spectrum and showed a peak at  $1000\text{ cm}^{-1}$ , related to Si-O-Al and Si-O-Si bonds. Similar findings were made in other studies [25, 27]. Also, a peak at  $875\text{ cm}^{-1}$  was seen due to the presence of calcium carbonate. Furthermore, Zhu *et al.* [17] showed that about 20% of the alkali-activated MIBA paste was C-S-H and pirssonite. The authors also showed that the chemical structure of C-S-H in the MIBA paste is similar to that of cement paste. However, the MIBA paste has a higher degree of silicate-chains' polymerization. According to XRD diffractograms, most of the crystalline phases in MIBA particles are quartz, calcite, magnetite and hydroxyapatite. After alkali activation process, other new peaks can be seen due to pirssonite C-(A)-S-H at  $29^\circ$  and  $50^\circ$ , and  $\text{Na}_2\text{Ca}(\text{CO}_3)_2 \cdot 2\text{H}_2\text{O}$  at  $34^\circ$ ,  $35^\circ$  and  $17^\circ$  (Figure 8). Additionally, Lancellotti *et al.* [25] concluded that reactive Si/Al ratio is an important parameter to be considered for a proper AAM formulation. Therefore, it is essential to determine the quantity of both amorphous Si and Al bearing phases in the precursor and the alkaline solutions. In addition, the same authors determined the quantity of potentially reactive aluminosilicate ( $\text{Al}_2\text{SiO}_5$ ) fraction in MIBA. The authors concluded that there is a significant difference between the reactive Si/Al ratio of the MIBA-based AAM due to the variability of crystalline and amorphous fractions with a different degree of reactivity. In addition, the total Si/Al ratio of the sample was between 2.5 and 3.5. According to the study of Davidovits [30], the physical characteristics of hardened geopolymer is significantly affected by the Si/Al ratio, and the mixture can be used in concrete when the ratio is lower than three.

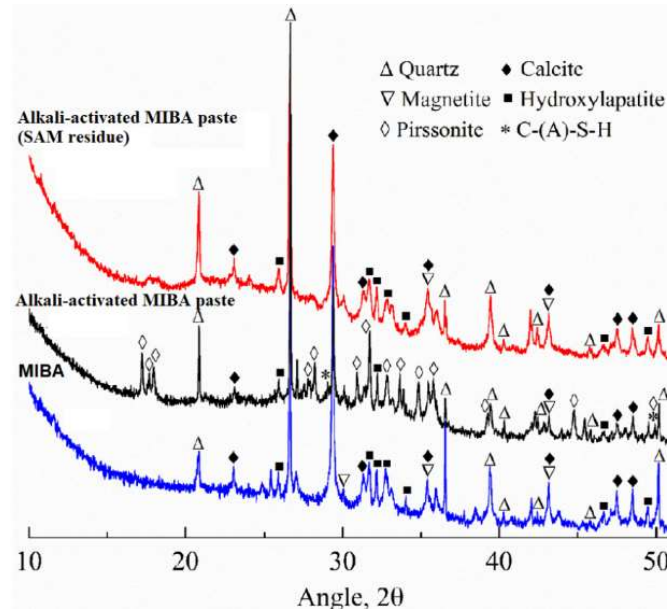


Figure 8 - XRD diffractograms of MIBA and alkali-activated MIBA paste [17]

### 3.5. Toxicity

Regarding alkali activated MIBA pastes and mortars, toxicity is one of the most studied characteristics (Table 1). Qiao *et al.* [11] and Garcia-Lodeiro *et al.* [12] showed that the solidification process of MIBA by alkali activation significantly decreases heavy metal leaching.

Chen *et al.* [13] concluded that both MIBA powder and alkali activated MIBA paste can be classified as non-hazardous waste materials at landfill based on the UK criteria. In addition, the concentration of the eluted metal parameters of MIBA powder are higher than the criteria of drinking water standard, while the concentration decreased for all the metal parameters in alkali activated MIBA paste, except for Cu and Cr. Similar conclusion were obtained by Rožek *et al.* [15].

Jing *et al.* [24] decreased the leaching potential and porosity of the alkali activated paste made with MIBA by using hydrothermal processing method under saturated steam pressure (1 MPa) at temperature of 180 °C for 12 hours.

According to the study of Krausova *et al.* [26], the results showed that the leaching rate of Cd increased after the heat treatment of MIBA. The opposite occurred for Pb.

Galiano *et al.* [14] also concluded that the heavy metals present in FA and MIBA can be stabilized with the use of alkali activation. Furthermore, Giro-Paloma *et al.* [3] showed that, apart from As, all the other results for heavy metal leaching are lower than that of the standard threshold specified for landfilling.

#### 4. Final remarks

The applicability of MIBA as solid precursor in the production of AAM depends solely on its chemical composition, which in turn depends on several factors related to the input MSW in incineration plants. Even though these ashes may present adequate, albeit extremely variable, amounts of silica and alumina, these are likely to be present in crystalline phases rather than amorphous ones, which significantly affects the ashes' reactivity. MIBA also typically presents a significant amount of metallic aluminium, which is not fully removed during the ashes' treatment process after incineration (via Eddy current separation). This component is the single most important factor negatively influencing the strength development of all AAM, via expansive reactions (hydrogen formation) in the plastic state leading to considerable porosity. Several methods have been proposed to eliminate these issues, by pressing the samples during compaction, increasing the mixing time to potentiate hydrogen reactions, heat treating the material, among others. Nonetheless, despite the aforementioned shortcomings, some have managed to use MIBA as the sole binder in AAM and achieve considerable mechanical performance, thus demonstrating its potential as an aluminosilicate precursor.

#### References

[1] Eurostat. Waste statistics in Europe. from [http://ec.europa.eu/eurostat/statistics-explained/index.php/Waste\\_statistics](http://ec.europa.eu/eurostat/statistics-explained/index.php/Waste_statistics). 2017.

- [2] Dhir R, de Brito J, Lynn C, Silva R. Sustainable construction materials: Municipal incinerated bottom ash. Cambridge, United Kingdom: Elsevier Science & Technology. Woodhead Publishing Series in Civil and Structural Engineering; 1 edition; 2017.
- [3] Giro-Paloma J, Maldonado-Alameda A, Formosa J, Barbieri L, Chimenos JM, Lancellotti I. Geopolymers based on the valorization of municipal solid waste incineration residues. IOP Conference Series: Materials Science and Engineering. 2017;251:012125.
- [4] Rowles M, O'Connor B. Chemical optimisation of the compressive strength of aluminosilicate geopolymers synthesised by sodium silicate activation of metakaolinite. J Mater Chem. 2003;13(5):1161-5.
- [5] Lancellotti I, Kamseu E, Michelazzi M, Barbieri L, Corradi A, Leonelli C. Chemical stability of geopolymers containing municipal solid waste incinerator fly ash. Waste Manage (Oxford). 2010;30(4):673-9.
- [6] Sacconi A, Sandrolini F, Andreola F, Barbieri L, Corradi A, Lancellotti I. Influence of the pozzolanic fraction obtained from vitrified bottom-ashes from MSWI on the properties of cementitious composites. Mater Struct. 2005;38(3):367-71.
- [7] Song Y, Li B, Yang E, Liu Y, Ding T. Feasibility study on utilization of municipal solid waste incineration bottom ash as aerating agent for the production of autoclaved aerated concrete. Cem Concr Compos. 2015;56:51-8.
- [8] Tang P, Florea M, Spiesz P, Brouwers H. Application of thermally activated municipal solid waste incineration (MSWI) bottom ash fines as binder substitute. Cem Concr Compos. 2016;70:194-205.
- [9] Bertolini L, Carsana M, Cassago D, Quadrio Curzio A, Collepardi M. MSWI ashes as mineral additions in concrete. Cem Concr Res. 2004;34(10):1899-906.
- [10] Qiao X, Tyrer M, Poon C, Cheeseman C. Characterization of alkali-activated thermally treated incinerator bottom ash. Waste Manage (Oxford). 2008a;28(10):1955-62.
- [11] Qiao X, Tyrer M, Poon C, Cheeseman C. Novel cementitious materials produced from incinerator bottom ash. Resour Conserv Recy. 2008b;52(3):496-510.
- [12] Garcia-Lodeiro I, Carcelen-Taboada V, Fernández-Jiménez A, Palomo A. Manufacture of hybrid cements with fly ash and bottom ash from a municipal solid waste incinerator. Constr Build Mater. 2016;105:218-26.

- [13] Chen Z, Liu Y, Zhu W, Yang E. Incinerator bottom ash (IBA) aerated geopolymer. *Constr Build Mater.* 2016;112:1025-31.
- [14] Galiano Y, Pereira C, Vale J. Stabilization/solidification of a municipal solid waste incineration residue using fly ash-based geopolymers. *J Hazard Mater.* 2011;185(1):373-81.
- [15] Rožek P, Król M, Mozgawa W. Solidification/stabilization of municipal solid waste incineration bottom ash via autoclave treatment: Structural and mechanical properties. *Constr Build Mater.* 2019;202:603-13.
- [16] Zhu W, Chen X, Struble L, Yang E. Feasibility study of municipal solid waste incinerator bottom ash as geopolymer precursor. *Fourth International Conference on Sustainable Construction Materials and Technologies.* Las Vegas, USA2016 p.
- [17] Zhu W, Chen X, Struble L, Yang E. Characterization of calcium-containing phases in alkali-activated municipal solid waste incineration bottom ash binder through chemical extraction and deconvoluted Fourier transform infrared spectra. *J Cleaner Prod.* 2018;192:782-9.
- [18] Zhu W, Chen X, Zhao A, Struble L, Yang E. Synthesis of high strength binders from alkali activation of glass materials from municipal solid waste incineration bottom ash. *J Cleaner Prod.* 2019;212:261-9.
- [19] Kim Y, Kang S. Characterization of geopolymer made of municipal solid waste incineration ash slag. *Journal of the Korean Crystal Growth and Crystal Technology.* 2014;24(1):15-20.
- [20] Wongsas A, Boonserm K, Waisurasingha C, Sata V, Chindaprasirt P. Use of municipal solid waste incinerator (MSWI) bottom ash in high calcium fly ash geopolymer matrix. *J Cleaner Prod.* 2017;148:49-59.
- [21] Huang G, Ji Y, Li J, Zhang L, Liu X, Liu B. Effect of activated silica on polymerization mechanism and strength development of MSWI bottom ash alkali-activated mortars. *Constr Build Mater.* 2019;201:90-9.
- [22] Huang G, Ji Y, Zhang L, Li J, Hou Z. The influence of curing methods on the strength of MSWI bottom ash-based alkali-activated mortars: The role of leaching of OH<sup>-</sup> and free alkali. *Constr Build Mater.* 2018;186:978-85.
- [23] Xuan D, Tang P, Poon C. MSWIBA-based cellular alkali-activated concrete incorporating waste glass powder. *Cem Concr Compos.* 2019;95:128-36.

- [24] Jing Z, Jin F, Yamasaki N, Ishida E. Hydrothermal synthesis of a novel tobermorite-based porous material from municipal incineration bottom ash. *Industrial & Engineering Chemistry Research*. 2007;46(8):2657-60.
- [25] Lancellotti I, Ponzoni C, Barbieri L, Leonelli C. Alkali activation processes for incinerator residues management. *Waste Manage (Oxford)*. 2013;33(8):1740-9.
- [26] Krausova K, Cheng T, Gautron L, Dai Y, Borenstajn S. Heat treatment on fly and bottom ash based geopolymers : Effect on the immobilization of lead and cadmium. *International Journal of Environmental Science and Development*. 2012;3(4):350-3.
- [27] Onori R, Will J, Hoppe A, Poletini A, Pomi R, Boccaccini A. Bottom ash-based geopolymer materials: Mechanical and environmental properties. In *Developments in Strategic Materials and Computational Design II* (eds W M Kriven, A L Gyekenyesi, J Wang, S Widjaja and D Singh)2011 p.
- [28] Liu Y, Sidhu K, Chen Z, Yang E. Alkali-treated incineration bottom ash as supplementary cementitious materials. *Constr Build Mater*. 2018;179:371-8.
- [29] Penilla R, Bustos A, Elizalde S. Zeolite synthesized by alkaline hydrothermal treatment of bottom ash from combustion of municipal solid wastes. *J Am Ceram Soc*. 2003;86(9):1527-33.
- [30] Davidovits J. Geopolymers - Inorganic polymeric new materials. *J Therm Anal*. 1991;37(8):1633-56.

Lisboa, May 21<sup>st</sup> 2019

Authors

Rawaz Kurda

PhD Researcher

Rui Vasco Silva

PhD Researcher

Jorge de Brito

Full Professor